Separation Science and Technology
Publication details, including instructions for authors and subscription information:
http://www.informaworld.com/smpp/title~content=t713708471

Counterdiffusion of Liquid Hydrocarbon Pairs in Ion-Exchanged Forms of Zeolite X

Ali Çulfaz[a]; Gönül Ergün[ab]
[a] Department of Chemical, Engineering Middle East Technical University, Ankara, Turkey [b] Aselsan Electronics Industry, Macunköy, Ankara, Turkey

To cite this Article Çulfaz, Ali and Ergün, Gönül(1986) 'Counterdiffusion of Liquid Hydrocarbon Pairs in Ion-Exchanged Forms of Zeolite X', Separation Science and Technology, 21: 5, 495 — 517
To link to this Article: DOI: 10.1080/01496398608056131
URL: http://dx.doi.org/10.1080/01496398608056131

SEPARATION SCIENCE AND TECHNOLOGY, 21(5), pp. 495-517, 1986

Counterdiffusion of Liquid Hydrocarbon Pairs in Ion-Exchanged Forms of Zeolite X

ALİ ÇULFAZ and GÖNÜL ERGÜN*

DEPARTMENT OF CHEMICAL ENGINEERING
MIDDLE EAST TECHNICAL UNIVERSITY
ANKARA, TURKEY

Abstract

Adsorptive counterdiffusion rates of liquid benzene, ethyl benzene, 1,3,5-trimethyl benzene, and 1-methyl naphthalene into Na^+, K^+, Cs^+, and Ca^{2+} ion exchanged forms of zeolite X saturated with cyclohexane were measured. The diffusivity of the adsorbing hydrocarbon decreases as the effective pore size of the zeolite is decreased by ion exchange. The effective pore size in CaX and CsX was so small as not to allow the adsorptive counterdiffusion of 1,3,5-trimethyl benzene and 1-methyl naphthalene. Diffusion took place only after the cations in the pore mouths were displaced to other cation sites in the structure under the influence of the adsorbing hydrocarbon molecules, and thus the rate of counterdiffusion appeared to increase with time.

INTRODUCTION

In most of the industrial applications of zeolites as adsorbents and catalysts, counterdiffusion of hydrocarbons takes place. The presence of diffusion limitations plays an important role in the processes using zeolites. A quantitative approach to the diffusivities of the species in systems similar to the ones in industrial applications is also needed.

Diffusion in zeolites is a complicated transport process. Diffusion rate is affected by the type and origin of the zeolite, shape and size of the diffusate, interaction between the zeolite and the diffusate, and the presence and amount of other molecules as well as temperature. No

---

*Present address: Aselsan Electronics Industry, Macunköy, Ankara, Turkey.

0149-6395/86/2105-0495$3.50/0

theoretical model taking into account the variables affecting the diffusion rate has yet been developed.

Information available on counterdiffusion in zeolites is limited. Counterdiffusion of some liquid hydrocarbon pairs was studied by Satterfield, Katzer, and co-workers in zeolite Y (*1–4*) and in mordenite (*5, 6*).

In the present study the adsorptive counterdiffusions of benzene, ethyl benzene, 1,3,5-trimethyl benzene, and 1-methyl naphthalene into several cation forms of zeolite X saturated with cyclohexane were investigated. The effects of adsorbate molecular size, effective pore size, and cation type of zeolite on the diffusion rate were studied.

EXPERIMENTAL

Materials

NaX sample was supplied in powder form by the Linde Division of Union Carbide (Lot 70117399). The crystal size was determined on the scanning electron micrograph. The average crystal diameter was 2.0 μm. Zeolite marked as HY-II was a sample of large single crystals of NaX synthesized by Dr H. Yücel according to the method of Charnell (*7*). The average diameter of these single crystals was 44 μm. The organic compounds used were examined by gas chromatography for impurities prior to their use. Purity was better than 99.9 wt% for all of the hydrocarbons.

Preparation of Ion-Exchanged Forms of Zeolite X

K^+, Ca^{2+}, and Cs^+ exchanged forms of zeolite X were prepared from the Na^+ form by using aqueous solutions of KNO_3, $Ca(NO_3)_2$, and CsCl, respectively, at 293 K. For K^+ and Ca^{2+} exchange, 10 g of NaX were added to 500 mL of 1 *M* KNO_3 and $Ca(NO_3)_2$ solutions, respectively, and for Cs^+ exchange 2 g of NaX and 0.2 *M* CsCl solution that initially contained twofold excess of the exchanging ion were used. With intermittent shaking the samples were left in the exchange solutions for 2 days. Solutions were filtered and washed with 50 mL of distilled water. Filtrates were analyzed by flame photometry for Na^+ content. Solids were dried at

323 K for 24 h. The entire exchange process was repeated once more in order for the ion exchange to be complete.

Na^+ analysis of the filtrates showed that K^+ and Ca^{2+} exchanges were 100% while Cs^+ exchange was 66 wt%. The results are in accord with previous work (*8*) reporting that the maximum degree of Cs^+ ion exchange is 0.65 to 0.80, and the Cs^+ ions with 0.169 nm ionic radius cannot replace the Na^+ ions that are in the hexagonal prisms (called Site I of the zeolite X framework) through the 0.24-nm apertures. The framework structure and the cation positions in the Na^+ form of zeolite X are shown in Fig. 1. The description of the cation positions is given in Table 1 (*9*).

Counterdiffusion Experiments

Experiments were performed in small glass ampules with a 8-cm^3 bulb and a capillary neck of about 9 cm length drawn from 0.3 cm diameter to

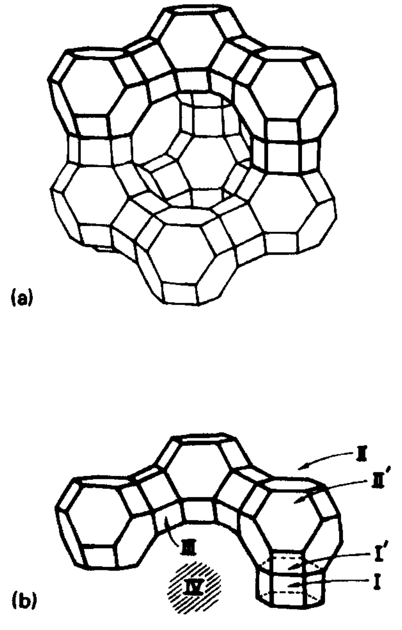

FIG. 1. (a) Framework structure of zeolite X. (b) Cation positions in the Na^+ form of zeolite X as indicated in reference to the part of the zeolite X framework drawn in heavy lines.

TABLE 1
Cation Positions in Zeolite X Structure

Position	Site	Sites per unit cell
Center of hexagonal prisms	I	16
In sodalite cage, adjacent to hexagonal prisms	I′	32
In supercage, adjacent to the six-ring outside of sodalite cage	II	32
In sodalite cage, adjacent to the single six-ring	II′	32
In supercage, neighborhood of the four-ring	III	48
In twelve-rings of supercage	IV	16

about 0.1 cm diameter at top. The zeolite samples were stored in a constant humidity desiccator. About 80 mg zeolite was filled into the ampule weighed to the nearest 0.1 mg. The ampule was placed in a container connected to a high vacuum line and a heater was placed such that the bottom part of the container was completely in it. The sample was heated slowly to 740 K at about 3 h and outgassed for 17 h at a pressure of about 2×10^{-4} mmHg. After outgassing, the container was disconnected from the vacuum line and the tip of the ampule was immediately sealed in the flame of a Bunsen burner. The ampule was weighed again to determine the weight of the outgassed zeolite sample.

The outgassed zeolite was saturated with cyclohexane by breaking the neck of the ampule and injecting immediately 1.5 mL of cyclohexane with a syringe. The ampule was closed with a glass stopper wrapped tightly by a strip of Teflon band. The ampule was left overnight for saturation.

Counterdiffusion experiments were done at 293 K. At the start of a run a predetermined amount of the second hydrocarbon, whose adsorptive counterdiffusion rate was to be measured, was injected in the ampule by a 10-μL syringe. A stopwatch was started and the contents of the ampule were mixed on a touch-plate. Mixing was stopped for about 20 s in order for the zeolite particles to settle before taking 1-μL samples for analysis by gas chromatography. A Packard Series 427 gas chromatograph with dual flame ionization detector was used with two glass columns of 4 mm inside diameter. The 6-ft long Column 1 contained 3% EGA liquid in the chromosorb GAW-DMSC support while the 1-ft long Column 2 was packed with support Gaschrom Q with 3% OV-1 as the liquid phase. The change in the concentration of the adsorbing species in the bulk liquid phase analyzed by gas chromatography was in the 0.1 to 1 wt% range.

ANALYSIS OF THE COUNTERDIFFUSION PROCESS

In the present study the counterdiffusion process was assumed to follow Fick's second law in spherical geometry for the component whose diffusion rate was measured. Analysis of the transient uptake curves obtained in sorption experiments with Fick's second law and proper initial and boundary conditions gives the effective diffusion coefficient. Spherical geometry is most appropriate for faujasite-type zeolites X and Y since diffusion occurs in three dimensions within the crystal lattice and the individual particles are compact, many-sided polyhedra which are best approximated by a sphere.

With the assumption that the diffusion coefficient is constant and diffusion occurs in the radial direction, the diffusion equation in spherical geometry reduces to the form

$$\frac{\partial C}{\partial t} = D\left(\frac{\partial^2 C}{\partial r^2} + \frac{2}{r}\frac{\partial C}{\partial r}\right)$$

Initial and boundary conditions for the case of adsorptive diffusion from a well-stirred solution of limited volume are as follows:

1. At zero time, the adsorbate concentration is zero within the particles
2. The adsorbate concentration profile is symmetrical about the center of the sphere at all times
3. The rate at which the adsorbate leaves the solution is always equal to the rate at which it enters the sphere at the surface for all times

The solution of this problem is given by Carman and Haul (*10*) and by Crank (*11*) as

$$\frac{M_t}{M_e} = 1 - \sum_{n=1}^{\infty} \frac{6\alpha(\alpha + 1)}{9 + 9\alpha + q_n^2\alpha^2} \exp\left(-\frac{Dq_n^2 t}{a^2}\right)$$

where q_n's are the nonzero, positive roots of

$$\tan q_n = \frac{3q_n}{3 + \alpha q_n^2}$$

α is the effective volume ratio of the solution to the sphere, and related to the final fractional uptake of adsorbate by

$$\text{final fractional uptake} = \frac{C_0 - C_f}{C_0} = \frac{1}{1 + \alpha}$$

Numerical values of M_t/M_e were calculated for $(Dt/a^2)^{1/2}$ between 0 and 0.200 at intervals of 0.001 and final fractional uptake between 0.50 and 0.99 at intervals of 0.01. Effective reduced diffusivity, D/a^2, of the adsorbing hydrocarbon in cyclohexane-saturated zeolite X was found by matching the $(Dt/a^2)^{1/2}$ values obtained from the solution of the diffusion equation with the experimental $t^{1/2}$ data at the same fractional approach to equilibrium.

RESULTS

Variation of the concentration of the hydrocarbon that was being adsorbed with time was determined in the bulk liquid phase. Fractional

TABLE 2
Adsorptive Counterdiffusion of 1-MN into NaX Saturated with Cyclohexane

Run 11
Amount of activated NaX: 0.0480 g
C_0: 7.81 × 10^{-3} g 1-MN/g solution of 1-MN in cyclohexane
C_f: 0.40 × 10^{-3} g 1-MN/g solution of 1-MN in cyclohexane
M_e: 0.15 g 1-MN adsorbed/g activated zeolite NaX
Final fractional uptake: 0.95

Time t (min)	Concentration of 1-MN in solution, $C_t \times 10^3$ (g/g)	Fractional approach to equilibrium (M_t/M_e)	$(Dt/a^2)^{1/2}$
0	7.81	0.0	—
1.05	6.65	0.157	0.0027
3.33	5.40	0.325	0.0065
5.62	5.10	0.366	0.0076
8.47	4.70	0.420	0.0094
11.5	4.20	0.487	0.0119
14.1	3.75	0.548	0.0148
17.1	3.45	0.588	0.0170
23.0	3.20	0.622	0.0192
32.3	2.55	0.710	0.0267
54.1	2.20	0.757	0.0325
180	0.70	0.960	0.139
1440	0.40	1.0	—

approach to equilibrium, M_t/M_e, corresponding to each time was calculated from the concentration data. Typical data are given in Table 2 for the adsorptive counterdiffusion of 1-MN into NaX saturated with cyclohexane. One set of data for the quantity of the counterdiffusing hydrocarbon adsorbed by zeolite X versus time are shown in Fig. 2 for 1-MN in Na^+, K^+, and Ca^{2+} forms of zeolite X. Plots of $(Dt/a^2)^{1/2}$ versus $t^{1/2}$ are given for each run in Figs. 3 to 10. Reduced diffusivities are found from the slopes of the linear portions by linear least squares fit.

Reduced diffusivities of the adsorbing hydrocarbons and the amounts adsorbed at equilibrium are summarized in Table 3. Reduced diffusivities are the averages of the runs performed with the same zeolite cation form-hydrocarbon pairs. Adsorbed amounts of the hydrocarbons at equilibrium are expressed in the following units: g hydrocarbon/g

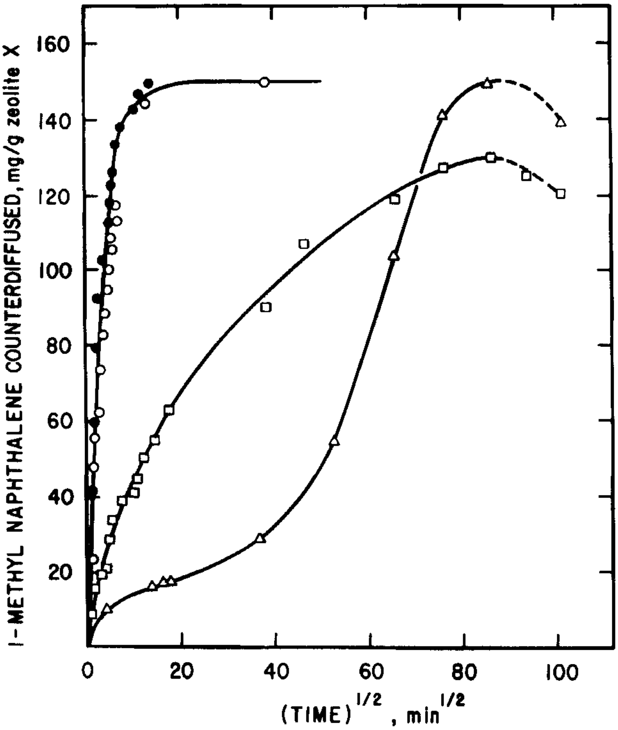

FIG. 2. Adsorptive counterdiffusion of 1-methyl naphthalene into several cation forms of cyclohexane-saturated zeolite X: (●) NaX, Run 10; (○) NaX, Run 11; (□) KX, Run 12; (△) CaX, Run 13.

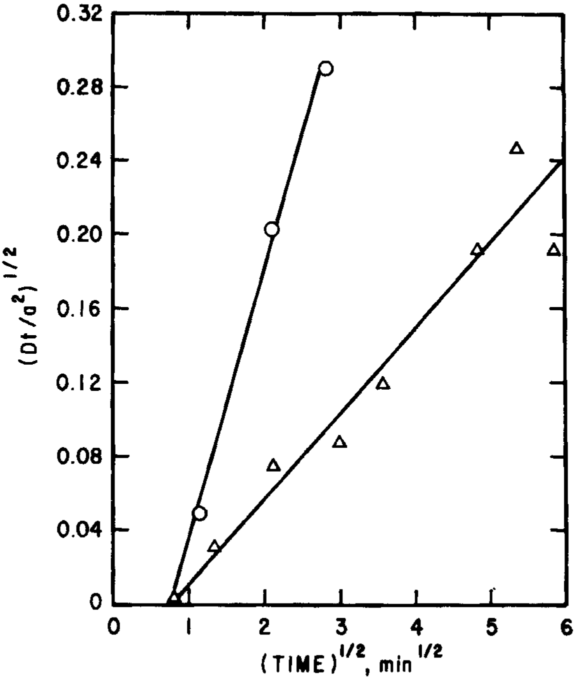

FIG. 3. Variation of $(Dt/a^2)^{1/2}$ with $t^{1/2}$ for adsorptive counterdiffusion of ethyl benzene into NaX saturated with cyclohexane: (○) Run 4, $D/a^2 = 3.4 \times 10^{-4}$ s^{-1}; (△) Run 5, $D/a^2 = 3.5 \times 10^{-5}$ s^{-1}.

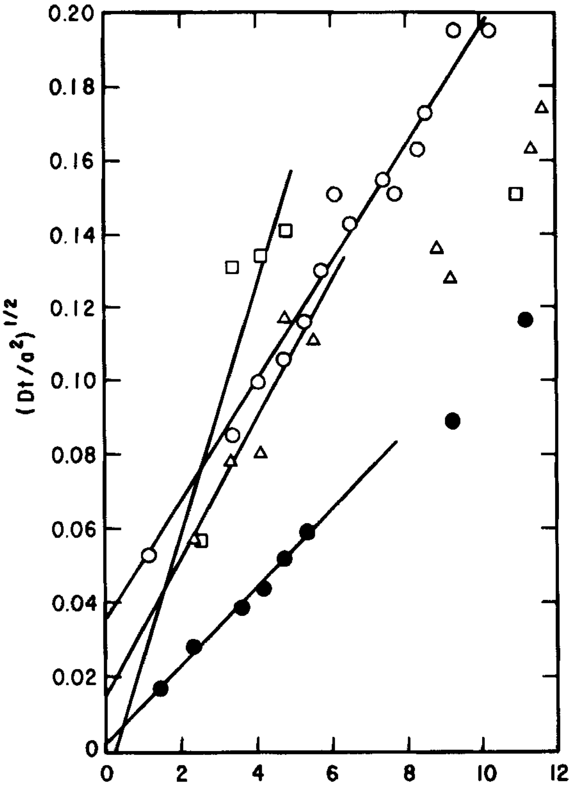

FIG. 4. Variation of $(Dt/a^2)^{1/2}$ with $t^{1/2}$ for adsorptive counterdiffusion of 1,3,5-trimethylbenzene into NaX saturated with cyclohexane: (○) Run 6, $D/a^2 = 4.4 \times 10^{-6}$ s^{-1}; (△) Run 7, $D/a^2 = 5.8 \times 10^{-6}$ s^{-1}; (□) Run 8, $D/a^2 = 1.9 \times 10^{-5}$ s^{-1}; (●) Run 9, $D/a^2 = 1.8 \times 10^{-6}$ s^{-1}.

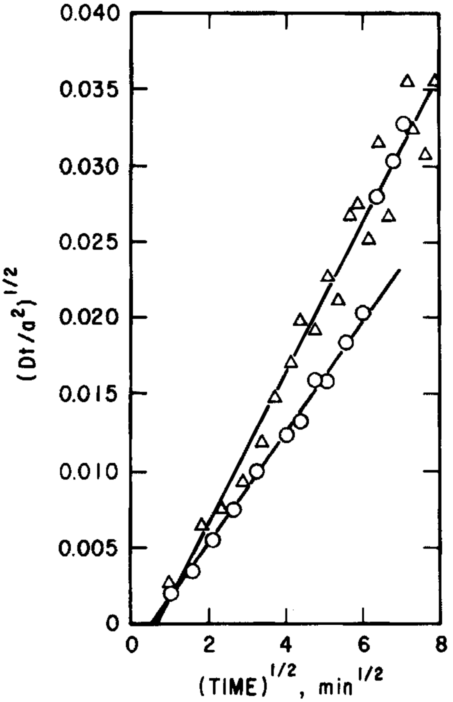

FIG. 5. Variation of $(Dt/a^2)^{1/2}$ with $t^{1/2}$ for adsorptive counterdiffusion of 1-methyl naphthalene into NaX saturated with cyclohexane: (○) Run 10, $D/a^2 = 2.2 \times 10^{-7}$ s^{-1}; (△) Run 11, $D/a^2 = 4.0 \times 10^{-7}$ s^{-1}.

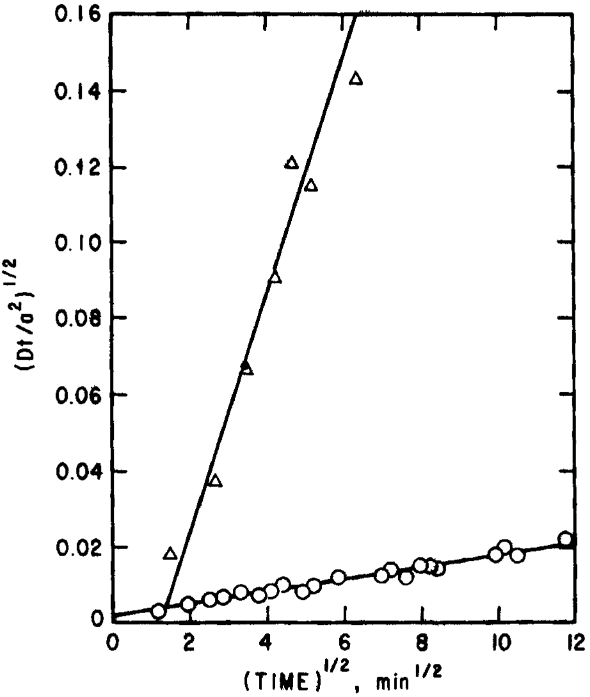

FIG. 6. Variation of $(Dt/a^2)^{1/2}$ with $t^{1/2}$ for adsorptive counterdiffusion of 1-methyl naphthalene (O, Run 12, $D/a^2 = 4.3 \times 10^{-8}$ s^{-1}) and 1,3,5-trimethyl benzene (Δ, Run 18, $D/a^2 = 1.7 \times 10^{-5}$ s^{-1}) into KX saturated with cyclohexane.

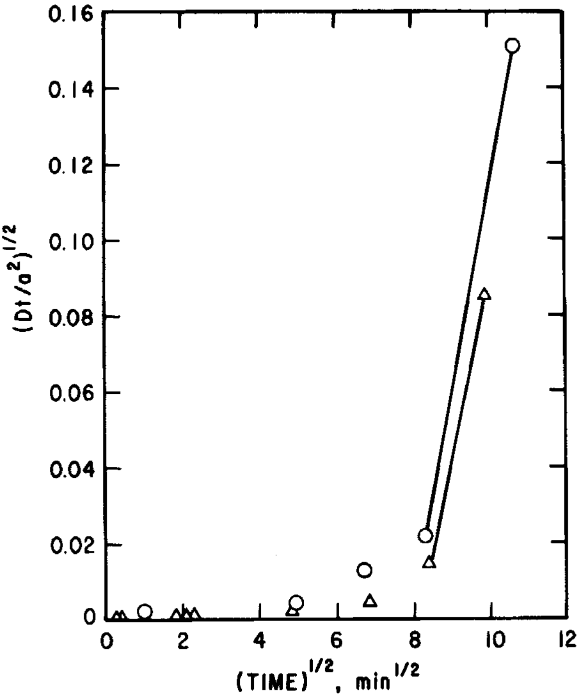

FIG. 7. Variation of $(Dt/a^2)^{1/2}$ with $t^{1/2}$ for adsorptive counterdiffusion of 1-methyl naphthalene (Δ, Run 13, $D/a^2 = 6.3 \times 10^{-7}$ s^{-1}) and 1,3,5-trimethyl benzene (O, Run 19, $D/a^2 = 8.1 \times 10^{-7}$ s^{-1}) into CaX saturated with cyclohexane.

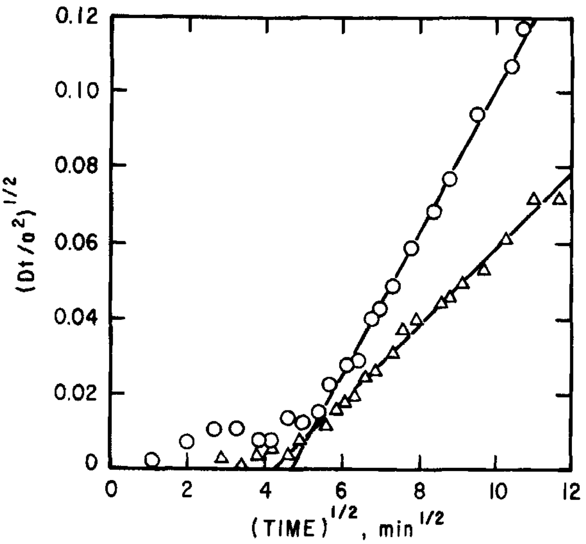

FIG. 8. Variation of $(Dt/a^2)^{1/2}$ with $t^{1/2}$ for adsorptive counterdiffusion of ethyl benzene into large crystals of NaX (HY-II) saturated with cyclohexane: (O) Run 14, $D/a^2 = 6.0 \times 10^{-6}$ s^{-1}; (Δ) Run 15, $D/a^2 = 1.7 \times 10^{-6}$ s^{-1}.

dehydrated zeolite, cm^3 hydrocarbon/g dehydrated zeolite, and molecules of hydrocarbon/cage of zeolite. Volume of the adsorbed hydrocarbons were calculated from liquid densities. Molecules per cage were calculated based on typical unit cell contents of zeolite X (*12*), and noting that there are eight cages per unit cell.

DISCUSSION

Selection of Cyclohexane as the Desorbing Hydrocarbon

When zeolite NaX was saturated with benzene and adsorptive counterdiffusion of cyclohexane was studied, no concentration change in the bulk liquid was observed after 1 day, whereas adsorptive counterdiffusion of benzene into cyclohexane-saturated zeolite NaX was essentially complete within an hour with an uptake of 0.12 g benzene/g dehydrated zeolite.

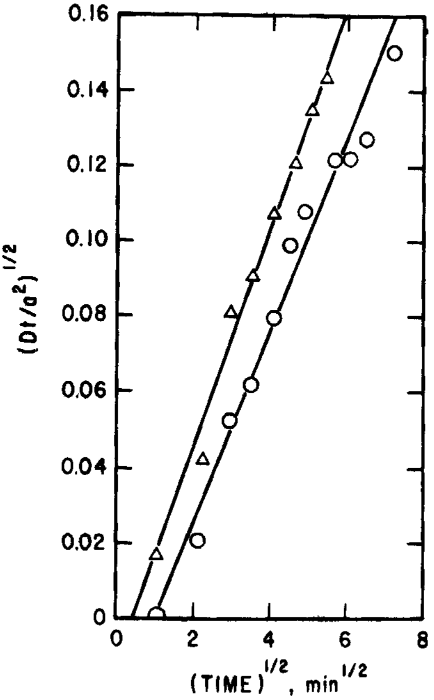

FIG. 9. Variation of $(Dt/a^2)^{1/2}$ with $t^{1/2}$ for adsorptive counterdiffusion of 1,3,5-trimethyl benzene into large crystals of NaX (HY-II) saturated with cyclohexane: (○) Run 16, $D/a^2 = 1.1 \times 10^{-5}\ s^{-1}$; (△) Run 17, $D/a^2 = 1.4 \times 10^{-5}\ s^{-1}$.

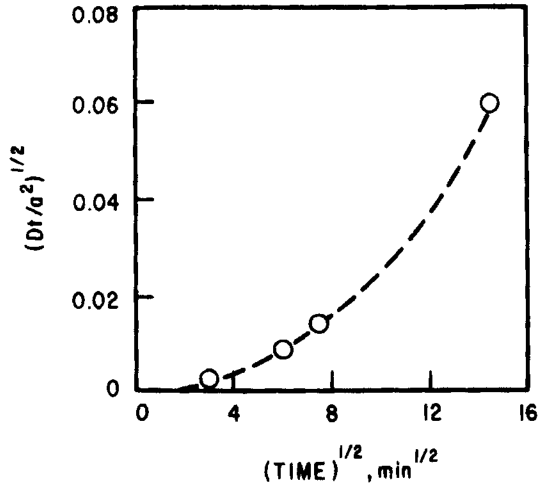

FIG. 10. Variation of $(Dt/a^2)^{1/2}$ with $t^{1/2}$ for adsorptive counterdiffusion of 1,3,5-trimethyl benzene into CsX saturated with cyclohexane.

In the study of adsorptive counterdiffusion rates of benzene, EB, 1,3,5-TMB, and 1-MN, cyclohexane was selected as the counterdiffusing species in all runs since the nature of the counterdiffusing species affected the diffusion rate of the compound of interest (*1*). The size and shape of cyclohexane are similar to the aromatic molecules studied, and aromatic compounds are preferentially adsorbed relative to cyclohexane because of their π-bonding structure.

Sorption at Constant Temperature and Negligible Bulk Phase Resistance

Isothermal sorption assumption made in the calculation of reduced diffusivities from uptake curves should be valid for the systems studied. Heat of adsorption of the hydrocarbon whose adsorptive counterdiffusion rate was measured was counterbalanced by the heat of desorption of cyclohexane. In addition, the liquid hydrocarbons provided higher heat transfer rates from zeolite particles to the surrounding liquid compared to adsorption from a gas phase at low pressures.

Diffusivity of benzene in cyclohexane in the bulk liquid phase at 293 K was estimated by the method of Wilke and Chang (*13*) to be 1.3×10^{-5}

TABLE 3

Diffusivities and Amounts of Hydrocarbons Adsorbed at Equilibrium in Adsorptive Counterdiffusion against Cyclohexane-Saturated Zeolite X at 293 K

Zeolite	Hydrocarbon diffusing in	Crystal radius a (μm)	Reduced diffusivity D/a^2 (s^{-1})	Effective diffusivity D (cm^2/s)	Amount adsorbed at equilibrium		
					g/g	cm^3/g	molecules/cage
NaX	Benzene	1.0	$>7 \times 10^{-4}$	$>7 \times 10^{-12}$	0.12	0.14	2.6
NaX	EB	1.0	1.9×10^{-4}	1.9×10^{-12}	0.11	0.12	1.7
NaX	1,3,5-TMB	1.0	7.8×10^{-6}	7.8×10^{-14}	0.10	0.12	1.4
NaX	1-MN	1.0	3.1×10^{-7}	3.1×10^{-15}	0.15	0.15	1.7
KX	1,3,5-TMB	1.0	1.7×10^{-5}	1.7×10^{-13}	0.07	0.08	1.1
KX	1-MN	1.0	4.3×10^{-8}	4.3×10^{-16}	0.13	0.13	1.7
CaX	1,3,5-TMB	1.0	8.1×10^{-7}	8.1×10^{-15}	0.09	0.10	1.2
CaX	1-MN	1.0	6.3×10^{-7}	6.3×10^{-15}	0.15	0.15	1.7
CsX	1,3,5-TMB	1.0	—	—	0.04	0.04	0.8
NaX (HY-II)	EB	22	3.9×10^{-6}	1.9×10^{-11}	0.12	0.14	1.9
NaX (HY-II)	1,3,5-TMB	22	1.3×10^{-5}	6.3×10^{-11}	0.07	0.09	1.0

cm^2/s. The reduced counterdiffusion coefficient, D/a^2, of benzene in cyclohexane saturated zeolite X crystals of 2 μm diameter was measured to be $7 \times 10^{-4}\ s^{-1}$. This is equivalent to a counterdiffusion coefficient, D, of $7 \times 10^{-12}\ cm^2/s$, which is much less than the bulk diffusion coefficient. Thus, the mass transfer resistance in the bulk liquid was negligible so that the mixing rate was not critical.

Attainment of Counterdiffusion Equilibrium

In the experiments the decrease in the concentration of the adsorbing hydrocarbon in the bulk liquid phase was measured. When the decrease had stopped, the concentration measured was taken to be the equilibrium concentration and this was checked at least the following day. In some of the systems a slight increase in the concentration of the adsorbing hydrocarbon was observed after reaching its minimum value. No evidence could be found of a reaction occurring in similar systems at the conditions of the experiment. For those cases, the minimum value was taken as the equilibrium concentration.

Effective Reduced Diffusivities of the Adsorbing Hydrocarbons in Cyclohexane-Saturated Zeolite X

Reduced diffusivities were found from the linear least squares fits of $(Dt/a^2)^{1/2}$ versus $t^{1/2}$ plots. In order to check the reproducibility of reduced diffusivities, four runs were performed for adsorptive counterdiffusion of 1,3,5-TMB into cyclohexane-saturated NaX. The results shown in Fig. 4 indicate that the reduced diffusivities are precise within one order of magnitude.

The counterdiffusion rate of benzene into cyclohexane-saturated NaX was so rapid that the first data point corresponded to a fractional uptake of about 0.8. The diffusion coefficient could be larger than the one obtained from that first data point, so the reduced diffusivity of this system was expressed as $>7 \times 10^{-4}\ s^{-1}$.

Effect of Molecular Size on Diffusion Rate

Critical molecular diameters of the hydrocarbons used in this study were calculated from bond lengths, bond angles, and van der Waals radii (*14*). The results are shown in Table 4.

TABLE 4
Critical Molecular Diameters

Hydrocarbon	Critical molecular diameter (nm)
Cyclohexane	0.69
Benzene	0.68
Ethyl benzene (EB)	0.68
1,3,5-Trimethyl benzene (TMB)	0.84
1-Methyl naphthalene (MN)	0.79

The dependence of effective diffusivity on the critical molecular diameter of the diffusate is shown in Fig. 11. The region in which most of the data of Moore and Katzer (*4*) fell for adsorptive counterdiffusion into cyclohexane-saturated NaY is also given in this figure. Effective diffusivity decreases exponentially as the critical molecular diameter is increased.

The reduced diffusivity of 1-MN (3.1×10^{-7} s^{-1}) was lower than that of 1,3,5-TMB (7.8×10^{-6} s^{-1}) although its molecular diameter is smaller. This behavior, which is contrary to the explanation by molecular sizes, can be attributed to the preferential adsorption of 1-MN by zeolite X as evidenced by its larger uptake (0.15 g/g for 1-MN against 0.10 g/g for 1,3,5-TMB). 1-MN has more π-bonding electrons which interact with the cations of the zeolite. Strong interactions between diffusing molecules and zeolite will lower the mobility of the diffusate within the zeolite channels.

Comparison with Previous Data

Adsorptive counterdiffusion of 1,3,5-TMB into cyclohexane-saturated NaY had been studied by Satterfield and Cheng (*3*) at 303 K and by Moore and Katzer (*4*) at 298 K. Structures of type X and type Y zeolites are the same. Reported values of effective diffusivities were 1.3×10^{-14} cm^2/s at 303 K (*3*) and 8×10^{-15} cm^2/s at 298 K (*4*). Effective diffusivity of 1,3,5-TMB into cyclohexane-saturated NaX obtained in this study was 7.8×10^{-14} cm^2/s at 293 K.

Unidirectional effective diffusivity of liquid 1,3,5-TMB in NaY at 303 K was reported by Satterfield and Cheng (*2*) as 7.2×10^{-12} cm^2/s which is two to three orders of magnitude higher than the counterdiffusion values

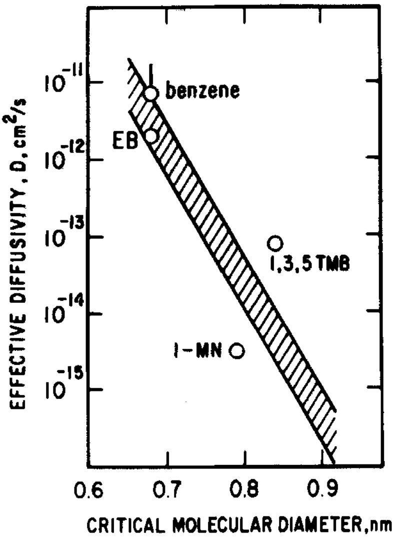

FIG. 11. Dependence of effective diffusivity on the critical molecular diameter of diffusate into the Na^+ form of zeolite X saturated with cyclohexane at 293 K. The results of Moore and Katzer (*4*) for the adsorptive counterdiffusion into the Na^+ form of zeolite Y (which has the same framework as zeolite X) saturated with cyclohexane at 298 K are shown in the shaded area.

in NaX or NaY summarized above. Molecule–molecule interactions between counterdiffusing species were expected to reduce the diffusion coefficient of a component relative to that observed in unidirectional diffusion.

Effect of Type of Cation in Zeolite on Diffusion Rate and Displacement of Cations by Diffusate Molecules

Ionic radii of Na^+, K^+, Cs^+, and Ca^{2+} are 0.095, 0.133, 0.169, and 0.099 nm, respectively (*14*). Counterdiffusion of 1,3,5-TMB and 1-MN were investigated in cyclohexane-saturated KX and CaX. The reduced diffusivity of 1,3,5-TMB in KX ($1.7 \times 10^{-5}\ s^{-1}$) was about the same as the one in NaX ($7.8 \times 10^{-6}\ s^{-1}$). For 1-MN, however, the reduced diffusivity in KX ($4.3 \times 10^{-8}\ s^{-1}$) was about one order of magnitude less than the reduced diffusivity in NaX ($3.1 \times 10^{-7}\ s^{-1}$). Since K^+ has a larger ionic radius than

Na^+, a reduction in pore size accompanied by a decrease in effective diffusion coefficient is expected.

Essentially no diffusion had occurred for 20 h in the desorptive counterdiffusion of 1,3,5-TMB and 1-MN into cyclohexane-saturated NaX. Diffusion of the adsorbing hydrocarbon started after 20 h, and the diffusion rate increased with time. Increasing slopes of $(Dt/a^2)^{1/2}$ versus $t^{1/2}$ plots, as shown in Fig. 7, indicated increasing reduced diffusivities. This behavior could be explained by the displacement of the Cs^+ cations in the structure from the pore mouths under the influence of the diffusate molecules.

In zeolite X, Ca^{2+} ions prefer Site I and Site II with no cation population in the higher sites (*9*). Site II cations are the main functional surface cations. Ca^{2+} ions resting on the free hexagonal faces of the sodalite units (Site II) were probably protruding into the main sorption cavity near the pore aperture. The presence of such cations could hinder the diffusion of molecules through the pore apertures. Increasing diffusion rates at larger times suggested that Ca^{2+} ions protruding into the pore apertures were forced by the diffusing molecules to other locations, probably within the supercage. Under these conditions 1,3,5-TMB and 1-MN were able to diffuse through the pore apertures.

A similar behavior was observed in adsorptive counterdiffusion of 1,3,5-TMB into Cs^+-exchanged zeolite X saturated with cyclohexane. The diffusion rate was very slow, and a diffusivity value increasing with time was suggested from the $(Dt/a^2)^{1/2}$ versus $t^{1/2}$ plot as shown in Fig. 10. Cs^+ ions which have a diameter of 0.169 nm were probably obstructing the main pore apertures and partly displaced to other sites under the influence of diffusate molecules. In that run the amount of 1,3,5-TMB adsorbed at equilibrium was 0.8 molecules/cage, indicating that not all cavities were available for the diffusate molecules to reach.

Effect of Crystal Size on Diffusion Rate

Adsorptive counterdiffusion of EB and 1,3,5-TMB into cyclohexane-saturated NaX crystals was determined for NaX preparations of largely different crystal sizes. Effective diffusivity, *D*, for EB was found to be 1.9×10^{-12} cm²/s for the commercial preparation of small crystals (2 μm diameter) of NaX, and 1.9×10^{-11} cm²/s for the large single crystals (44 μm diameter) of NaX prepared according to the Charnell (*7*) method. If the effective diffusivity is constant, the reduced diffusivity should decrease with the square of the crystal size. The reduced diffusivities for EB were 1.9×10^{-4} and 3.9×10^{-6} s^{-1} for the small and large crystals of NaX, respectively. However, the effective diffusivity of 1,3,5-TMB was found to be 7.8×10^{-14} cm^2/s for the small crystals of NaX and 6.3×10^{-11} cm^2/s for the large crystals so that the reduced diffusivities for the small and large crystals were nearly the same (7.8×10^{-6} s^{-1} for small crystals and 1.3×10^{-5} s^{-1} for large crystals, respectively). Orders of magnitude differences in diffusivities are not uncommon when the zeolite samples are of different origin. However, the amounts adsorbed at equilibrium are the same on both small and large crystals of NaX for 1,3,5-TMB (0.07 g/g zeolite) and very nearly the same for EB (0.11 g/g zeolite NaX for small crystals, and 0.12 g/g zeolite NaX for large crystals).

CONCLUSIONS

Adsorptive counterdiffusion rates of hydrocarbon pairs in zeolite X are affected by the molecular size of the adsorbate, the effective pore size of the zeolite, and the type of cation present in the zeolite framework. Reduced diffusivity of the adsorbing hydrocarbon decreases exponentially with increasing molecular diameter for similar diffusates in the framework of the Na^+ form of zeolite X.

The size and nature of cations in the zeolite framework have a significant effect on the diffusion rate. The counterdiffusion rate is lowered by decreasing the effective pore size of zeolite X as the Na^+ cations are exchanged with K^+. In the Ca^{2+} and Cs^+ ion-exchanged forms of zeolite X, the effective pore size was so small as not to allow the adsorptive counterdiffusion of 1,3,5-TMB and 1-MN. The occurrence of diffusion after several hours is due to the displacement of Site II cations in the pore apertures to other sites under the influence of diffusate molecules.

Diffusion in zeolites is a very complicated transport process. Although it is known that type, origin, and effective pore size of zeolite, type of cation present in zeolite, and molecular size and nature of the diffusate affect the diffusion rate, differences in diffusivities of the apparently same systems cannot always be explained by these variables. More systematic studies in simple systems are needed to understand the effect of each variable and to develop theoretical models of counterdiffusion in zeolites.

SYMBOLS

a	characteristic diffusion length, or particle radius (cm)
C	concentration of the adsorbing hydrocarbon in the bulk liquid phase (g adsorbate/g cyclohexane)
C_f	concentration at equilibrium
C_0	concentration at time zero
C_t	concentration at time t
D	effective diffusivity of adsorbate (cm^2/s)
D/a^2	effective reduced diffusivity of adsorbate (s^{-1})
EB	ethyl benzene
M_t	amount of adsorbate having diffused in at time t (g adsorbate in zeolite/g cyclohexane in the bulk liquid phase)
M_e	amount of adsorbate having diffused in at equilibrium (g adsorbate in zeolite/g cyclohexane in the bulk liquid phase)
M_t/M_e	fractional approach to equilibrium (dimensionless)
1-MN	1-methyl naphthalene
t	time (s)
1,3,5-TMB	1,3,5-trimethyl naphthalene
α	effective volume ratio of the solution to the sphere (dimensionless)

Acknowledgment

We thank Dr H. Yücel for providing us with the large single crystals of NaX.

REFERENCES

1. C. N. Satterfield and J. R. Katzer, *Adv. Chem. Ser.*, *102*, 193 (1971).
2. C. N. Satterfield and C. S. Cheng, *AIChE Symp. Ser. No. 117*, *67*, 43 (1971).
3. C. N. Satterfield and C. S. Cheng, *AIChE J.*, *18*, 724 (1972).
4. R. M. Moore and J. R. Katzer, *Ibid.*, *18*, 816 (1972).
5. C. N. Satterfield, J. R. Katzer, and W. R. Vieth, *Ind. Eng. Chem., Fundam.*, *10*, 478 (1971).
6. C. N. Satterfield and G. T. Chiu, *AIChE J.*, *20*, 522 (1974).
7. J. F. Charnell, *J. Cryst. Growth*, *8*, 291 (1971).
8. D. W. Breck, *Zeolite Molecular Sieves*, Wiley, New York, 1974, p. 542.
9. Ref. *8*, pp. 97–105.

10. P. C. Carman and R. A. W. Haul, *Proc. R. Soc. London, Ser. A, 222*, 109 (1954).

11. J. Crank, *The Mathematics of Diffusion*, Oxford University Press, London, 1956, pp. 88–90.

12. Ref. *8*, p. 176.

13. C. R. Wilke and P. Chang, *AIChE J., 1*, 264 (1955).

14. L. Pauling, *The Nature of the Chemical Bond*, 3rd ed., Cornell University Press, Ithaca, New York, 1960, p. 514.

Received by editor August 6, 1985